[1]I. Freund, Opt. Commun. (to be published); a brief account of some aspects of this process is given here.

[2]Coherent three-quantum processes are discussed by (a) I. Freund and B. F. Levine, Phys. Rev. Lett. **23**, 854 (1969); Phys. Rev. Lett. **25**, 1241 (1970); (b) P. Eisenberger and S. L. McCall, Phys. Rev. Lett. **26**, 684 (1971); Phys. Rev. A **3**, 1145 (1971); (c) S. S. Jha and J. W. F. Woo, Phys. Rev. B **5**, 4210 (1972); J. W. F. Woo and S. S. Jha, Phys. Rev. B **6**, 4081 (1972); S. S. Jha and J. W. F. Woo, Nuovo Cimento B **10**, 229 (1972).

[3]Incoherent three-quantum processes are discussed by B. F. Levine and I. Freund, Opt. Commun. **3**, 197 (1971).

[4]Resonant three-quantum processes are discussed by I. Freund and B. F. Levine, Opt. Commun. **3**, 101 (1971).

[5](a) G. Breit and E. Teller, Astrophys. J. **91**, 215 (1940); (b) J. Shapiro and G. Breit, Phys. Rev. **113**, 179 (1959); (c) L. Spitzer and J. L. Greenstein, Astrophys. J. **114**, 407 (1951); (d) W. Zernik, Phys. Rev. **132**, 320 (1963); Phys. Rev. **133**, A117 (1964); Phys. Rev. **135**, A51 (1964); (e) B. Honig and J. Jortner, J. Chem. Phys. **47**, 3698 (1967); (f) S. Klarsfeld, Phys. Lett. **30**, 382 (1969); (g) P. Braunlich and P. Lambropoulos, Phys. Rev. Lett. **25**, 135 (1970); Phys. Rev. Lett. **25**, 986 (1970); Phys. Rev. A **5**, 1013 (1972); (h) W. R. Johnson, Phys. Rev. Lett. **29**, 1123 (1972); (i) J. M. Wessner, D. K. Anderson, and R. T. Robiscoe, Phys. Rev. Lett. **29**, 1126 (1972); (j) H. R. Reiss, Phys. Rev. A **6**, 817 (1972); Phys. Rev. A **1**, 803 (1970); Phys. Rev. D **4**, 3533 (1971).

[6](a) R. Novick, in *Physics of One- and Two-Electron Atoms*, edited by F. Bopp and H. Kleinpoppen (North-Holland, Amsterdam, 1969), pp. 296–325; (b) M. Lipeles, R. Novick, and N. Tolk, Phys. Rev. Lett. **15**, 690 (1965); (c) C. J. Artura, N. Tolk, and R. Novick, Astrophys. J. Lett. **157**, L181 (1969); (d) C. A. Kocher, J. E. Clendenin, and R. Novick, Phys. Rev. Lett. **29**, 615 (1972); (e) M. H. Prior, Phys. Rev. Lett. **29**, 611 (1972); (f) R. C. Elton, L. J. Palumbo, and H. R. Griem, Phys. Rev. Lett. **20**, 783 (1968); (g) R. Marrus and R. W. Schmieder, Phys. Rev. A **5**, 1160 (1972), and references to earlier work by these authors contained herein.

[7]O. Bely, J. Phys. B **1**, 718 (1968).

[8]M. Göppert-Mayer, Ann. Phys. (Leipzig) **9**, 273 (1931).

[9]M. Ianuzzi, Phys. Rev. Lett. **13**, 371 (1964).

[10]N. Bloembergen, *Nonlinear Optics* (Benjamin, New York, 1965), Chaps. 2–8.

[11]W. L. Peticulas, R. Morris, and K. E. Rieckhoff, J. Chem. Phys. **42**, 4164 (1965).

[12]I. Freund (unpublished).

[13]P. A. M. Dirac, *The Principles of Quantum Mechanics* (Oxford U.P., London, 1958), Sec. 63.

[14]*International Tables for X-Ray Crystallography* (Kynoch, Birmingham, England, 1965), Vol. III, Sec. 3.2.

[15]R. W. James, *The Optical Principles of the Diffraction of X-Rays* (Cornell U.P., Ithaca, N.Y., 1965), Chap. IV.

[16]P. Lambroulos, Phys. Rev. **168**, 1418 (1969).

PHYSICAL REVIEW A VOLUME 7, NUMBER 6 JUNE 1973

Auger Spectra of Carbon and Argon Following Ionization by Equal-Velocity α Particles and Deuterons*

R. L. Watson

Department of Chemistry and Cyclotron Institute, Texas A&M University, College Station, Texas 77843

L. H. Toburen

Battelle, Pacific Northwest Laboratories, Richland, Washington 99352

(Received 26 December 1972)

The spectra of carbon K- and argon L-shell Auger electrons resulting from ionization produced by 0.15–0.50-MeV/amu α particles and deuterons incident on a thin gas cell have been measured. Absolute ionization cross sections were obtained from the Auger-electron yields and, in addition, the yields obtained with equal-velocity projectiles were used to test the projectile z dependence of the ionization process. Intense satellite structure was observed in the Auger spectra and these features were attributed to Auger transitions from multiple vacancy states formed during the collision.

I. INTRODUCTION

Several measurements have been reported[1,2] in which comparisons of x-ray yields resulting from equal-velocity α-particle and deuteron or proton bombardments have been used to test the theoretical prediction[3,4] that K-shell ionization cross sections are directly proportional to the square of the projectile charge. Significant deviations from the expected dependence have been deduced on the assumption that the fluorescence yields (which relate x-ray production cross sections to ionization cross sections) are the same for a given target element, regardless of the type of projectile being used to produce the ionization. It has recently been discovered, however, that even in collisions involving relatively light ions, such as α particles and protons, appreciable L-shell ionization frequently accompanies the production of a K-shell vacancy.[5–7] Since the fluorescence yields for multiply ionized states are expected to differ from those for singly ionized states, the assumption that the fluorescence yield is independent of the exciting particle could lead to erroneous results, especially for light elements where the effects of multiple ionization may result in a relatively large change in

fluorescence yield.[8] Furthermore, x-ray yield measurements are subject to errors resulting from the critical absorption of x rays emitted from multiply ionized atoms in which the binding-energy increases are sufficient to shift the x rays above an absorption edge.[6,8]

The above difficulties relating to the use of measured x-ray yields to deduce ionization cross sections are not encountered in converting measured Auger-electron yields to ionization cross sections for low-Z elements where fluorescence yields are very small. The present work was undertaken primarily for the purpose of testing the projectile Z dependence of K-shell ionization cross sections for carbon and L-shell ionization cross sections for argon by comparing the Auger yields obtained in bombardments with equal-velocity α particles and deuterons. Absolute ionization cross sections were also measured and are presented herein. Additional information relating to multiple ionization by α particles and deuterons was obtained from an analysis of the satellite structure appearing in the measured Auger spectra.

II. EXPERIMENTAL METHOD

α-particle and deuteron beams with energies of 0.150–0.500 MeV/amu were obtained by means of a Van de Graaff generator. Since the rf ion source used in the Van de Graaff accelerator has a very low efficiency for the production of He^{++} ions, the α-particle beam was produced by the gas stripping of an accelerated He^{+} beam. The accelerated He^{+} beam entered a gas-stripping cell after magnetic identification, and a second analyzing magnet was used following the stripping cell to separate the α particles from other products of charge transfer. This method of magnetic separation with intermediate stripping is also effective in removing unwanted beam contamination, such as H_2^{+} ions, which might otherwise be associated with the α-particles beam. The gas-stripping cell used in this work was approximately 7 m long and was operated at a pressure of about 2×10^{-5} torr. These conditions produced optimum stripping of the primary beam with minimal loss in beam intensity owing to gas scattering.

The deuteron beam was produced by accelerating D^{+} and using the same magnetic analysis described above for α particles. The gas-stripping region was evacuated to approximately 1×10^{-6} torr when D^{+} beams were used. Energy analysis of electrons ejected from D^{+} collisions with the target gas under study showed no evidence of electrons associated with H_2^{+} breakup. This result indicated that H_2^{+} contamination of the D^{+} beam, if any, was negligible.

The basic experimental technique for the measurement of electron-emission cross sections has

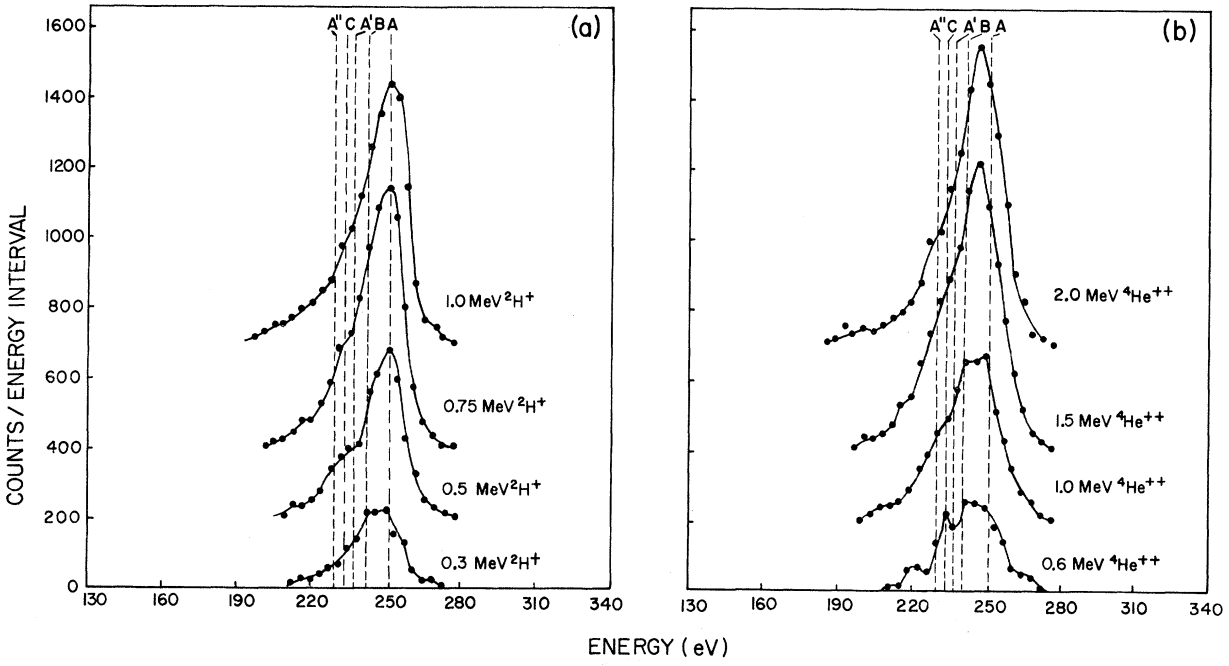

FIG. 1. Carbon K-shell Auger-electron spectra for deuterons and α particles incident on C_2H_6. The dashed lines labeled A, A′, and A″ indicate the expected positions of the normal $1s$-$2p2p$, $1s$-$2s2p$, and $1s$-$2s2s$ Auger transitions, respectively. The other dashed lines indicate the calculated positions of some of the possible satellite transitions listed in Table III.

been described in detail previously.[9] The incident beam is collimated and directed through a differentially pumped target-gas cell. Electrons ejected by ion-atom or ion-molecule interactions pass through a slit in the target cell, are energy analyzed by a cylindrical-mirror electrostatic analyzer, and are detected by a continuous channel electron multiplier. The energy resolution of the electrostatic analyzer used in the present work was 3.5% full width at half-maximum (FWHM). The energy calibration of the electrostatic analyzer was accomplished by comparison of the Auger spectra of ethane, argon, and neon with those measured by Moddeman,[10] Carlson and Krause,[11] and Edwards and Rudd,[12] respectively. The energy scale used in our work should be accurate to better than 1.0%. Research-grade target gases were used with impurities of less than 4 parts in 10^4.

III. DATA ANALYSIS AND RESULTS

A. Ionization Cross Sections

The spectra obtained in the present measurements are shown in Figs. 1 and 2. Auger yields were determined from the measured spectra by integrating the areas under the Auger-electron peaks. Before these peak integrations were carried out, backgrounds based on the electron continua on each side of the Auger peaks were subtracted. After correcting the Auger yields for solid angle, electron absorption, and analyzer transmission (as discussed in Ref. 9), ionization cross sections were computed on the basis of isotropic emission of Auger electrons. K-shell Auger-electron emission resulting from K-shell vacancy production by proton impact has previously been shown to be isotropic.[9] Nonisotropic angular distributions are theoretically possible for Auger transitions following the creation of a vacancy having quantum number $j > \frac{1}{2}$,[13,14] and a small anisotropy has, in fact, been observed by Cleff and Mehlhorn[15] for the $L_3M_{2,3}M_{2,3}(^1S_0)$ transition resulting from electron impact ionization of argon. Volz and Rudd,[16] however, have measured angular distributions for several L_3MM transitions in argon excited by 300-keV protons, and did not find any significant deviations from isotropy. As has already been noted, radiative transitions fill less than 0.5% of the primary carbon K-shell and argon L-shell vacancies, and hence correction for this competitive mode of decay is not required.

The cross sections obtained in the present study

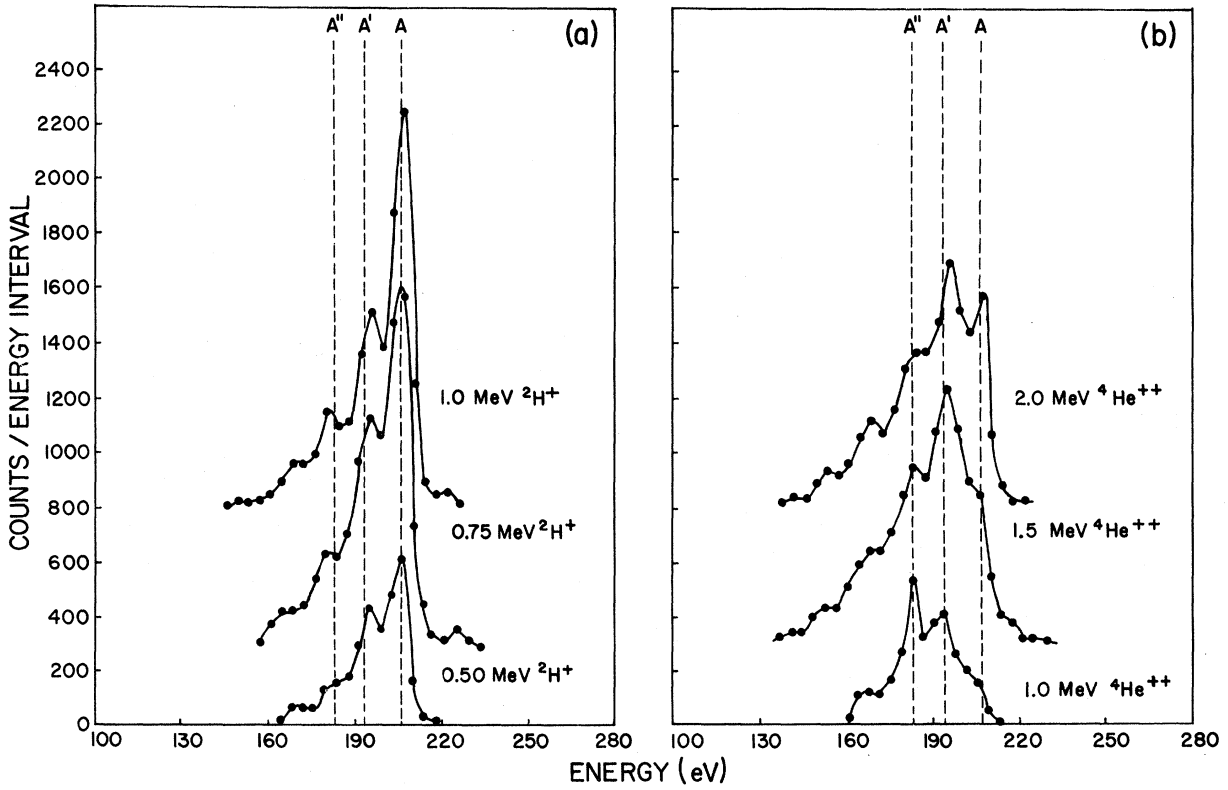

FIG. 2. L-shell Auger-electron spectra for deuterons and α particles incident on argon. The dashed lines labeled A, A′, and A″ indicate the expected positions of the normal $2p$-$3p3p$, $2p$-$3s3p$, and $2p$-$3s3s$ Auger transitions, respectively.

TABLE I. Cross sections for carbon K-shell and argon L-shell ionization by α particles and deuterons (in units of 10^{-18} cm^2).[a]

E/M (MeV/amu)	Carbon (K shell) α particles	deuterons	Argon (L shell) α particles	deuterons
0.150	1.57	0.35		
0.250	3.34	0.66	7.61	1.96
0.375	5.20	1.05	12.5	2.73
0.500	4.96	1.10	15.0	3.18

[a]Absolute errors are estimated to be ± 20%.

for carbon K-shell ionization and argon L-shell ionization by equal-velocity α particles and deuterons are listed in Table I. The uncertainties in the absolute values are estimated to be ± 20%.

Presented in Table II are the ratios $N_\alpha/4N_d$, where N_α and N_d are the Auger yields obtained with equal-velocity α particles and deuterons, respectively. Because the Auger yields for α particles and deuterons were measured under nearly identical conditions, these yield ratios are subject to far fewer uncertainties than are the absolute cross sections.

Since the number of particles passing through the target was determined from the integrated current produced in a Faraday cup, any projectiles which were not fully stripped of their electrons would cause the measured Auger cross sections to appear larger than they actually are. The switching magnet located approximately 3 m upstream from the target chamber ensured that the projectiles were fully stripped at that point, but, during their flight from the switching magnet to the Faraday cup, charge-changing collisions could occur with residual gas molecules in the beam line and target-gas molecules in the target chamber. Calculations based upon charge-changing cross sections given by Allison[17] indicated that this effect was important only for the 600-keV α-particle measurements, where it was found that under the conditions of the present experiment approximately 15% of the He^{++} beam ended up as He^{+} in the Faraday cup. As a result of this correction (which has been included in the values listed in Tables I and II), the 150-keV/amu Auger-electron yield ratio is considerably more uncertain than the rest.

B. Satellite Structure

An examination of the carbon K-shell Auger spectra shown in Fig. 1 reveals various structural changes in the gross features which appear to depend both on the type and energy of the projectile. In particular, the main peak is observed to be shifted about 4 eV down in energy in the spectra obtained with α particles as compared to the spectra obtained with deuterons. The differences in the structural features of the Auger spectra for the two types of particles become increasingly apparent as the bombarding energy decreases.

In comparing the features of the argon L-shell Auger spectra shown in Fig. 2, considerably more pronounced differences in structure are found. Especially striking is the abrupt reduction of the intensity of the high-energy peak in going from deuterons to α particles.

Effects similar to those described above have also been observed recently by Stolterfoht[18] in K-shell Auger spectra obtained by proton impact on N_2, CO_2, and CH_4. He attributes the changes in Auger structure to satellite peaks associated with double-vacancy production during the collision. This interpretation is consistent with evidence provided by x-ray measurements[5,19] which show that simultaneous K- plus L-shell ionization does indeed occur with substantial probability in light-ion collisions with intermediate- and low-Z atoms.

Referring back to Figs. 1 and 2, the normal transitions (i.e., the usual transitions associated with an initial *single*-vacancy configuration) are labeled with the letters A, A′, and A″. These letters correspond to the $1s$-$2p2p$, $1s$-$2s2p$, and $1s$-$2s2s$ transitions, respectively, for carbon and to the $2p$-$3p3p$, $2p$-$3s3p$, and $2p$-$3s3s$ transitions, respectively, for argon. The energies of the normal Auger transitions were taken from Moddeman[10] and Siegbahn *et al.*[20] in the case of carbon (CH_4 and C_2H_6), and from Carlson and Krause[11] in the case of argon.

In an effort to identify the various structural features of the measured Auger spectra as satellites associated with specific Auger transitions, Hartree-Fock-Slater calculations were carried out with the program of Herman and Skillman.[21] Energies of the KLL Auger transitions for carbon atoms and the LMM transitions for argon atoms, both in various multiply ionized initial configurations, were obtained from the differences in calculated total energies for initial and final states. The absolute transition energies calculated for free carbon atoms were not expected to accurately represent the measured Auger satellites for molecular C_2H_6. The energy *differences* between the normal transitions and their corresponding multi-

TABLE II. Auger-electron yield ratios for equal-velocity α particles and deuterons incident on carbon and argon.

E/M (MeV/amu)	$N\alpha/4Nd$ Carbon (K shell)	Argon (L shell)
0.150	1.13 ± 0.12	
0.250	1.25 ± 0.07	0.96 ± 0.05
0.375	1.24 ± 0.07	1.14 ± 0.06
0.500	1.13 ± 0.06	1.18 ± 0.06

TABLE III. Auger energies for *KLL* transitions in multiply ionized carbon atoms.

	Transition	Energy (eV) Measured[a] E	Calculated[b] ΔE	Calculated[b] E
A	$1s\text{-}2p2p(1s^{-1})$	250	0	250
B	$(1s^{-1},2s^{-1})$		−10	240
C	$(1s^{-1},2s^{-2})$		−16	234
	$(1s^{-2})$		22	272
A′	$1s\text{-}2s2p(1s^{-1})$	237	0	237
	$(1s^{-1},2s^{-1})$		−9	228
	$(1s^{-1},2p^{-1})$		−9	228
	$(1s^{-1},2s^{-1},2p^{-1})$		−14	223
A″	$1s\text{-}2s2s(1s^{-1})$	230	0	230
	$(1s^{-1},2p^{-1})$		−9	221
	$(1s^{-1},2p^{-2})$		−13	217

[a]Measured energies are for CH_4 from Refs. 10 and 20.
[b]ΔE is calculated energy difference between satellite transition and corresponding normal transition. E is transition energy obtained by adding ΔE to the measured energy of the appropriate normal transition.

ple-ionization satellites, however, should be nearly the same for C_2H_6 molecules as for free carbon atoms. The satellite energies were estimated by subtracting the calculated energy differences from the measured energies of the appropriate normal transitions. The results of the calculations for carbon are summarized in Table III. In this table the initial-state configuration is identified by indicating the number of vacancies in each level beyond those in the ground-state configuration. The letters preceding some of the transitions in Table I are used to identify the positions of these lines in Fig. 1.

The absolute transition energies calculated for the normal *LMM* transitions in argon were within 1 or 2 eV of the measured energies as given by Carlson and Krause.[11] The results of the calculations for the argon satellite transitions are summarized in Table IV. Additional analysis of the argon spectra was accomplished by fitting a series of Gaussian peaks having widths determined by the experimental spectrometer resolution to each spectrum. This procedure enabled a fairly accurate determination of the area of the peak corresponding to the normal $2p\text{-}3p3p$ transition (peak A in Fig. 2). Using this peak area and the intensities of the other "normal" transitions relative to the intensity of the $2p\text{-}3p3p$ transition as obtained from Carlson and Krause,[11] the normal Auger spectrum was subtracted from each of the measured spectra. The result of this analysis is shown in Fig. 3 for the Auger spectrum obtained with 2-MeV α particles. The letters in this figure indicate the expected locations of a few of the satellite transitions listed in Table IV. In this manner the total yields of Auger electrons associated with satellite transitions could be estimated. The ratios of the residual Auger yields (after subtrac-

TABLE IV. Auger energies for *LMM* transitions in multiply ionized argon atoms.

	Transition	Energy (eV) Measured[a] E	Calculated[b] ΔE	Calculated[b] E
A	$2p\text{-}3p3p(2p^{-1})$	206	0	206
B	$(2p^{-1},3p^{-1})$		−9	197
C	$(2p^{-1},3p^{-2})$		−20	186
	$(2p^{-1},3p^{-3})$		−32	174
	$(2p^{-2})$		10	216
A′	$2p\text{-}3s3p(2p^{-1})$	191	0	191
D	$(2p^{-1},3p^{-1})$		−12	179
E	$(2p^{-1},3p^{-2})$		−23	168
	$(2p^{-1},3p^{-3})$		−35	156
A″	$2p\text{-}3s3s(2p^{-1})$	180	0	180
F	$(2p^{-1},3p^{-1})$		−12	168
G	$(2p^{-1},3p^{-2})$		−24	156
	$(2p^{-1},3p^{-3})$		−36	144

[a]Measured energies from Ref. 11.
[b]ΔE is the calculated energy difference between the satellite transition and the corresponding normal transition. E is transition energy obtained by adding ΔE to the measured energy of the appropriate normal transition.

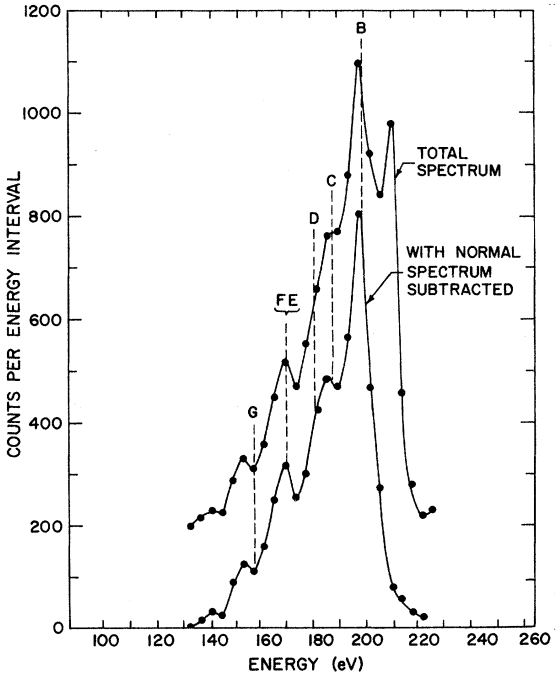

FIG. 3. Total and residual *L*-shell Auger-electron spectra for 2.0-MeV α particles incident on argon. The dashed lines indicate the calculated positions of some of the possible satellite transitions listed in Table IV.

TABLE V. Residual-to-total L-shell Auger-electron yield ratios for argon.

E/M (MeV/amu)	N_R/N_T Deuterons	α particles
0.250	0.40	0.83
0.375	0.38	0.74
0.500	0.36	0.67

tion of the normal spectra) to the total Auger yields are given in Table V.

IV. DISCUSSION

A. Ionization Cross Sections

The K-shell ionization cross sections for carbon obtained in the present work are compared with the results of other thin-target measurements in Fig. 4. They are plotted as a function of the velocity ratio $v_p/\bar{v}_K$, where v_p is the projectile velocity and $\bar{v}_K$ is the average K-shell electron velocity [$\bar{v}_K = (2U_K/m)^{1/2}$ and U_K is the K-shell binding energy]. The cross sections given by Harrison *et al.*[22] were deduced from x-ray measurements for protons on CH_4. Those given by Toburen[23,24] and by Stolterfoht[18] were derived from Auger-electron measurements. Toburen's values are averages for protons incident on CH_4, C_2H_6, and C_2H_2, whereas Stolterfoht's values are for protons incident on CH_4. Although different molecular environments affect the Auger yields to some extent, a previous study of carbon Auger yields obtained for different molecular forms of carbon showed the magnitude of this effect to be of the order of 5% or less for CH_4 and C_2H_6.[24]

The cross sections for deuterons incident on C_2H_6 obtained in the present work overlap quite well with the proton values obtained by the other investigators except at higher velocity ratios, where the present results along with the previous results of Toburen are about 20% higher than those of Stolterfoht. The cross sections obtained with α particles (divided by z^2) are systematically higher than the cross sections for deuterons throughout the range of velocity ratios measured.

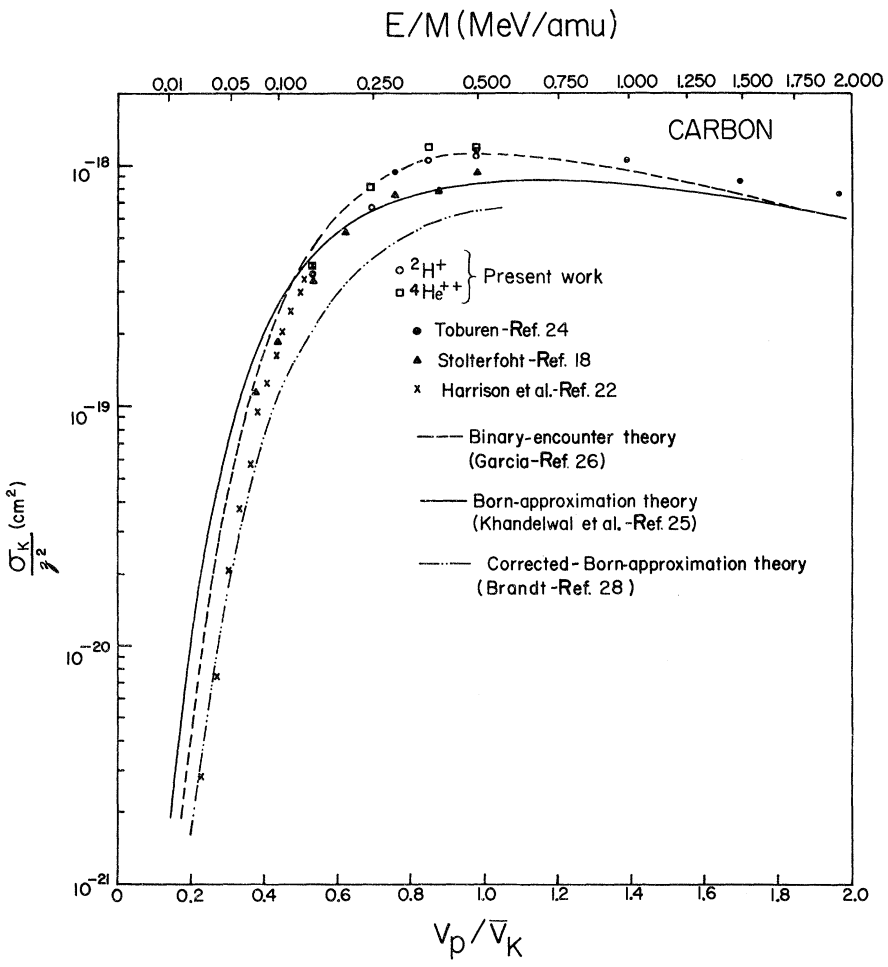

FIG. 4. Comparison of carbon K-shell ionization cross sections measured for thin targets with the predictions of various theories. The K-shell ionization cross section divided by the square of the projectile charge is plotted vs the projectile to K-shell electron velocity ratio where $\bar{v}_K = (2u_K/m)^{1/2}$ (u_K is the K-shell binding energy, 283 eV).

The solid and dashed curves in Fig. 4 show the predictions of the Born-approximation theory from tabulations given by Khandelwal *et al.*[25] and the predictions of the classical binary-encounter theory as presented by Garcia,[26] respectively. Similar comparisons have already been discussed in some detail by the above-mentioned experimenters, and so we restrict ourselves here to only a few brief observations regarding the over-all trends. In general, both theoretical approaches appear to give satisfactory agreement with the experimental results for protons above a velocity ratio of approximately 0.5. For $0.5 < v_p/\bar{v}_K < 2.0$ it is not clear from the experimental data which of the two theoretical descriptions gives the best results, but in any case the differences between them are only about 25% at most in this velocity range.

Below $v_p/\bar{v}_K \simeq 0.5$, both theories appear to overestimate the cross sections, with the binary-encounter theory overestimating by the smaller amount. Brandt *et al.*[27] have attributed the discrepancies between experimental cross sections and those calculated in the Born approximation at low velocity ratios to an increased binding of the K-shell electrons resulting from the close proximity of the projectile during the collision. Using the prescription given by Brandt,[28] we have corrected the Born-approximation cross sections for this binding effect and the results are shown by the dot-dashed curve in Fig. 4. (The Coulomb correction also discussed by Brandt[28] is negligible over this range of velocity ratios.) It is seen that this curve falls considerably below the experimental points at high velocity ratios, but it joins the

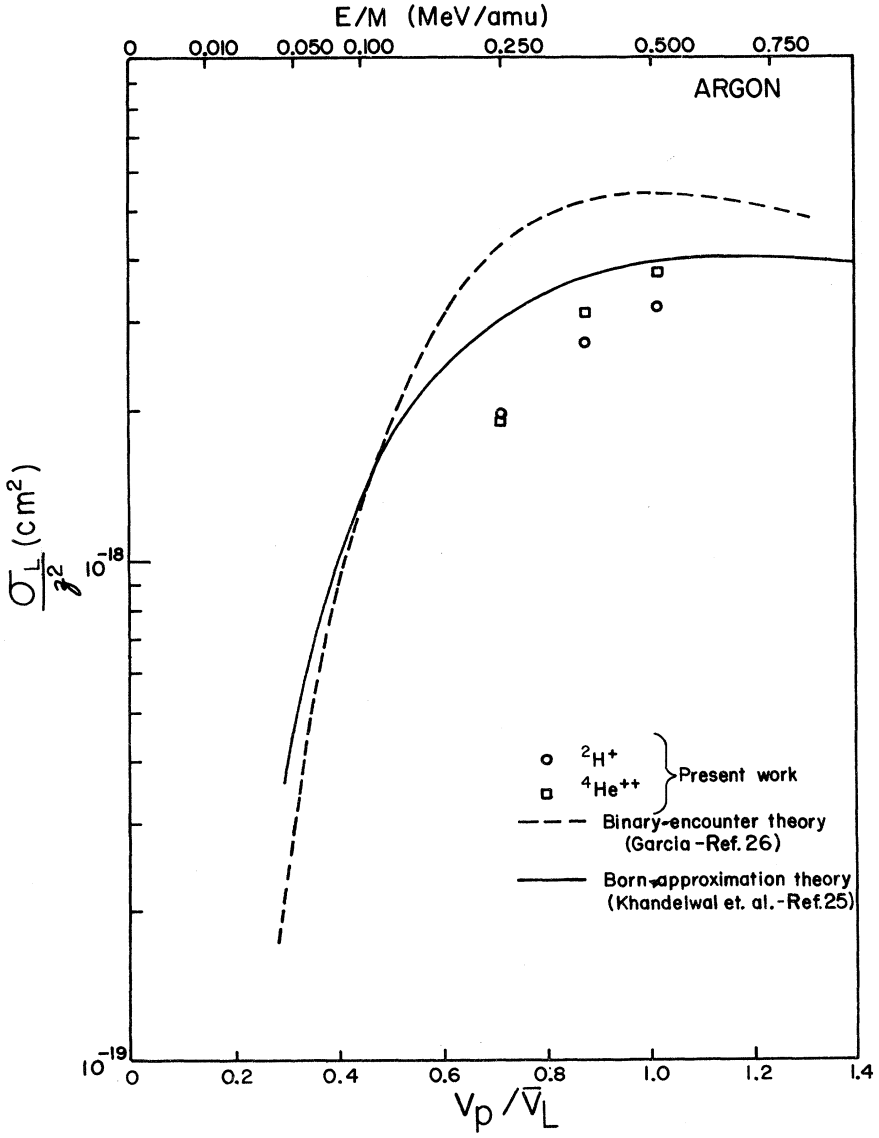

FIG. 5. Comparison of the argon L-shell ionization cross sections with the predictions of the binary-encounter and Born-approximation theories. The L-shell ionization cross section divided by the square of the projectile charge is plotted vs the projectile to L-shell electron velocity ratio where $\bar{v}_L = (2\bar{u}_L/m)^{1/2}$ ($\bar{u}_L$ is the average L-shell binding energy, 264 eV).

experimental points of Harrison *et al.*[22] at low velocity ratios. This underestimation of experimental results at the higher velocity ratios has been noted by Brandt,[28] and he and his co-workers[1] have developed a possible explanation for this in terms of a polarization effect.

The results of the L-shell ionization cross-section measurements for argon are shown in Fig. 5 along with the predictions of the Born-approximation and binary-encounter theories. It is apparent that fairly large discrepancies exist between the experimental and theoretical L-shell ionization cross sections at low velocity ratios. The experimental results appear to be converging with the Born-approximation curve at high velocity ratios.

B. Projectile Z Dependence

As was stated in Sec. I, one of the principal objectives of this study was to test the projectile Z dependence in the light-element region using Auger-electron yields. By comparing Auger yields instead of x-ray yields, as has been done in all previous studies,[1,2] uncertainties associated with the fluorescence yields are eliminated. A comparison of the Auger yields for carbon and argon in the form of a plot of the cross-section ratios $\sigma_\alpha/4\sigma_d$ as a function of the projectile energy per amu is shown in Fig. 6. If the predicted z^2 dependence were to be upheld, the experimental points would lie along the dashed line at $\sigma_\alpha/4\sigma_d = 1$. Rather large deviations are observed from a z^2 dependence for both K-shell ionization of carbon and L-shell ionization of argon.

To be consistent with the results of the above-mentioned x-ray measurements, the z^2 deviation should exhibit a crossover behavior in which the ratios are smaller than unity at low projectile velocities, rise above unity at higher velocities, and, finally, decrease back toward unity at the highest velocities. The present results do indeed follow this trend. The theory of Basbas *et al.*[1] contends that the crossover phenomenon occurs as a result of the exact cancellation of the binding effect (which acts to decrease the ionization cross section) and the polarization effect (which acts to increase the ionization cross section). This cancellation is expected to occur for n-shell ionization when

$$1/q_0 a_n \simeq 1 , \tag{1}$$

where $\hbar q_0$ is the minimum momentum transfer for n-shell ionization given by

$$\hbar q_0 = U_n/v_p , \tag{2}$$

and a_n is the Bohr radius of the n shell (corrected for inner-electron screening):

$$a_n = n^2\hbar^2/mZ_n e^2 . \tag{3}$$

In the above equations, U_n, v_p, m, and Z_n are the n-shell binding energy, projectile velocity, electron mass, and screened nuclear charge, respectively. Equation (3) can be rewritten in terms of the Bohr velocity of an n-shell electron (corrected for inner-electron screening) v_n to give

$$a_n = n^3 v_n \hbar/2Z_n^2 R , \tag{4}$$

where R is the Rydberg constant. Combining Eqs. (1), (2), and (4) results in the following expression for the crossover-point condition:

$$v_p/v_n = \tfrac{1}{2} n(n^2 U_n/Z_n^2 R) = \tfrac{1}{2} n\theta_n . \tag{5}$$

The crossover-point condition expressed in terms of the velocity ratio used throughout this paper

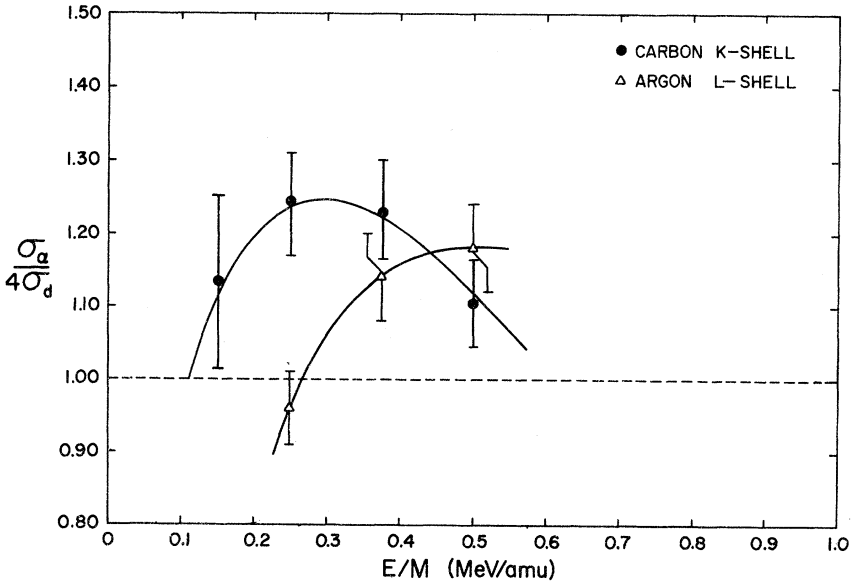

FIG. 6. Ionization cross-section ratio plotted vs the projectile energy per amu for carbon K shell and argon L shell. The behavior of this ratio for an exact z^2 dependence is shown by the dashed line.

$[v_p/\bar{v}_n$ where $\bar{v}_n \equiv (2U_n/m)^{1/2}]$ is obtained by noting that

$$v_n/\bar{v}_n = \frac{(2Z_n^2 R/n^2 m)^{1/2}}{(2U_n/m)^{1/2}} = \theta_n^{-1/2} . \quad (6)$$

Substituting this expression into Eq. (5), the final result is

$$v_p/\bar{v}_n = \tfrac{1}{2} n \theta_n^{1/2} . \quad (7)$$

The crossover point given by Eq. (7) occurs at $v_p/\bar{v}_K = 0.401$ for carbon ($E/M = 83$ keV/amu) and at $v_p/\bar{v}_L = 0.636$ ($E/M = 194$ keV/amu) for argon. Unfortunately, the large uncertainty in the 150-keV/amu point for carbon does not permit a conclusive experimental determination of the crossover velocity ratio. Based upon the present data, about all one can say in this regard is that a crossover should occur somewhere around $v_p/\bar{v}_K = 0.44$ ($E/M = 100$ keV/amu). In the case of argon, it is noted that the observed crossover velocity ratio is 0.75 ($E/M = 270$ keV/amu), which is 18% larger than the velocity ratio given by Eq. (7).

In summary, we have shown that large deviations from a z^2 dependence occur for carbon K-shell ionization and argon L-shell ionization, and that these deviations are not a result of variations in fluorescence yields. Although the present results are unable to accurately establish the crossover velocity ratio for carbon, it is apparent that the general trend of the projectile z dependence of carbon K-shell ionization cross sections is similar to that observed for argon L-shell ionization and to the trends deduced previously in K x-ray measurements with Cl, Ca, Ti, and Ni targets.[2]

C. Satellite Structure

In Sec. III B it was noted that evidence of satellite structure associated with Auger transitions from atoms which had undergone multiple ionization during the collision process appears in the measured carbon KLL and argon LMM Auger-electron spectra. In this section we concern ourselves with identifying the origins of the various structural features seen in these Auger spectra.

Carbon. Unfortunately, in the case of the KLL Auger spectra for carbon (Fig. 1), the broad widths of the various lines preclude very conclusive statements regarding satellite identities on the basis of our data alone. These linewidths are not solely a consequence of our experimental resolution but are characteristic of C_2H_6, even in very-high-resolution spectra.[20] In comparing our spectra for C_2H_6 with Stolterfoht's spectra for CH_4, however, it becomes apparent that the shift in the main peak energy in going from deuterons to α particles results from a substantial increase in the intensity of the satellite peak appearing at an energy of approximately 243 eV (peak B′) in Stolterfoht's spectra. Referring back to the calculated satellite peak energies in Table III, the most likely candidate appears to be the $1s$-$2p2p$ satellite transition associated with an initial double-vacancy-state configuration of $1s^{-1}2s^{-1}$ and having a calculated energy of 241 eV. The $1s$-$2p2p$ satellite transition for an initial vacancy-state configuration $1s^{-1}2p^{-1}$ would not be possible for a free carbon atom since only two $2p$ electrons are initially available. However, since we are dealing with carbon atoms bound in a molecule (C_2H_6), in effect, six $2p$ electrons are available and a $1s$-$2p2p$ satellite transition for an initial-state configuration of $1s^{-1}2p^{-1}$ would be expected to occur. In such a case this satellite line would occur at approximately the same energy as the one originating from a $1s^{-1}2s^{-1}$ initial configuration and may, in fact, be the dominant transition contributing to the observed satellite peak. The estimated position of the transition associated with an initial $1s^{-1}2s^{-1}$ or $1s^{-1}2p^{-1}$ vacancy is indicated by the dashed line labeled B in Fig. 1 and, as can be seen in the spectra obtained with 1.0- and 0.6-MeV α particles, coincides nicely with the observed structure.

Also, plainly visible in the Auger spectrum obtained with 0.6-MeV α particles (in Fig. 1) is a peak at approximately 234 eV. The energy of this peak corresponds to the energy calculated for the $1s$-$2p2p$ satellite transition associated with an initial triple-vacancy-state configuration of $1s^{-1}2s^{-2}$ (or $1s^{-1}2p^{-2}$). The position of this transition is indicated by the dashed line labeled C in Fig. 1.

We conclude, then, that the dominant features contributing to our Auger spectra for carbon (besides the "normal" Auger transitions) are associated with $1s$-$2p2p$ transitions arising from initial states having one and two vacancies in the $2s$ or $2p$ level in addition to a $1s$ vacancy. The relative intensities of these satellite transitions increase both as the projectile charge increases and as the projectile velocity decreases.

Argon. The residual Auger-electron spectrum (after subtraction of the "normal" spectrum) for 2.0-MeV α particles on argon (Fig. 3) shows significant structural features at 195, 183, 168, and 152 eV. Comparing these energies with the calculated energies for argon LMM satellites in Table IV, it is found that these energies correspond most closely to $2p$-$3p3p$, $2p$-$3s3p$, and $2p$-$3s3s$ satellite transitions associated with initial-state configurations having one and two vacancies in $3s$ or $3p$ levels in addition to a $2p$ vacancy. (Although Table IV only gives transition energies for $3p$ vacancies, they are the same within 2 eV for $3s$ vacancies.) The calculated positions of these transitions are indicated by the dashed lines in Fig. 3. In this fig-

ure it is seen that the calculated energy for transition G is somewhat higher than the structural feature appearing at 152 eV but, for the most part, the other indicated satellite energies coincide fairly well with the residual Auger structure.

If one makes the assumption that multiple-vacancy production in light-ion collisions is simply a result of simultaneous collisions with individual electrons during the ions' passage through the atom then one is led to expect that the cross section for the production of multiple vacancies is proportional to the product of the cross sections for producing each vacancy individually.[5] Thus if σ_n is the total cross section for n-shell ionization (irrespective of what other ionization is produced simultaneously) and if $\sigma_{n'}$ is defined similarly for the n' shell, then it follows that the total cross section for simultaneously producing *at least* one n-shell and one n'-shell vacancy is

$$\sigma_{nn'} \simeq c\sigma_n \sigma_{n'} , \tag{8}$$

where c is a proportionality constant, or

$$\frac{\sigma_{nn'}}{\sigma_n} \propto \sigma_{n'} . \tag{9}$$

The above result has been tested by Knudson, Burkhalter, and Nagel[5] for simultaneous K- plus L-shell ionization produced by protons incident on Al, and by Li, Watson, and Hansen[19] for simultaneous K- plus L-shell ionization produced by deuterons and α particles incident on Ca, Ti, and Fe. The former group found that the projectile velocity dependence of the K- plus L-shell cross-section ratio was correctly given by the L-shell ionization cross-section velocity dependence as calculated in the Born approximation. The latter group compared the same ratio with the L-shell cross-section velocity dependence predicted by the classical theory of Gryzinski[4] and found similar agreement.

In the present case of argon, Eq. (9) predicts that the L- plus M-shell to L-shell ionization cross-section ratio should follow the velocity dependence of the M-shell cross section. The ratios of the residual-to-total Auger yields given in Table V are estimates of the above cross-section ratio. We have compared the projectile velocity dependence of these ratios with the M-shell ionization cross-section velocity dependence as predicted by the Gryzinski model and find satisfactory agreement. It should be noted that this simple picture of multiple ionization predicts that σ_{LM}/σ_L should approximately follow a z^2 dependence on projectile charge. In Table V it is seen that the present results for deuterons and α particles only differ by about a factor of 2 instead of the factor of 4 required by a z^2 dependence.

In summary then, we have shown that most of the dominant features of the *LMM* Auger-electron spectra resulting from light-ion collisions with argon atoms are explainable in terms of satellite transitions associated with initial states having one or more vacancies in $3s$ or $3p$ levels. This conclusion was reached on the basis of (a) the correspondence between the observed structure and the calculated satellite transition energies, and (b) the agreement between the observed velocity dependence of the residual Auger yield with that predicted by the simple independent-collision picture of multiple ionization.

ACKNOWLEDGMENTS

The authors would like to thank L. L. Nichols, W. A. Glass, J. E. Choate, and C. A. Ratcliffe for their help in overcoming the many problems encountered in obtaining α particles with the positive-ion Van de Graaff accelerator. One of us (RLW) gratefully acknowledges travel support provided by the Northwest College and University Association for Science.

*Work supported by the U.S. Atomic Energy Commission.

[1]George Basbas, Werner Brandt, Roman Laubert, Anthony Ratowski, and Arthur Schwarzschild, Phys. Rev. Lett. **27**, 171 (1971); G. Basbas, W. Brandt, and R. Laubert, Phys. Lett. **34**, 277 (1971).

[2]C. W. Lewis, R. L. Watson, and J. B. Natowitz, Phys. Rev. A **5**, 1773 (1972).

[3]E. Merzbacher and H. W. Lewis, in *Encyclopedia of Physics*, edited by S. Flügge (Springer, Berlin, 1957), Vol. 34, p. 166.

[4]Michal Gryziński, Phys. Rev. **138**, A336 (1964).

[5]A. R. Knudson, P. G. Burkhalter, and D. J. Nagel, in *Proceedings of the International Conference on Inner-Shell Ionization Phenomena, Atlanta,* 1972, Conf.-720404 (USAEC, Oak Ridge, Tenn., 1973), Vol. 3, p. 1675.

[6]J. S. Hansen, T. K. Li, and R. L. Watson, in Ref. 5, p. 1682.

[7]C. F. Moore, M. Senglaub, B. Johnson, and P. Richard, Phys. Lett. **40**, 107 (1972).

[8]L. H. Toburen and F. P. Larkins, Phys. Rev. A **6**, 2035 (1972).

[9]L. H. Toburen, Phys. Rev. A **3**, 216 (1971).

[10]W. I. Moddeman, Oak Ridge National Laboratory Report No. ORNL-TM-3012 (1970), p. 125 (unpublished).

[11]T. A. Carlson and M. O. Krause, Phys. Rev. Lett. **17**, 1079 (1966).

[12]A. K. Edwards and M. E. Rudd, Phys. Rev. **170**, 140 (1968).

[13]W. Mehlhorn, Phys. Lett. **26**, 166 (1968).

[14]S. Flügge, W. Mehlhorn, and V. Scmidt, Phys. Rev. Lett. **29**, 7 (1972).

[15]B. Cleff and W. Mehlhorn, Phys. Lett. **37**, 3 (1971).

[16]D. J. Volz and M. E. Rudd, Phys. Rev. A **2**, 1395 (1970).

[17]S. K. Allison, Rev. Mod. Phys. **30**, 1137 (1958).

[18]N. Stolterfoht, in Ref. 5, Vol. 2, p. 1043.

[19]T. K. Li, R. L. Watson, and J. S. Hansen, Phys. Rev. A (to be published).

[20]K. Siegbahn, C. Nordling, G. Johansson, J. Hedman, P. F. Heden, K. Hamrin, U. Gelius, T. Bergmark, L. O. Werme, R. Manne, and Y. Baer, *ESCA Applied to Free Molecules* (North-Holland, Amsterdam, 1969), p. 103.

[21]F. Herman and S. Skillman, *Atomic Structure Calculations* (Prentice-Hall, Englewood Cliffs, N.J., 1963).
[22]K. G. Harrison, H. Tamara, and F. J. deHeer, Phys. Rev. A (to be published).
[23]L. H. Toburen, in Ref. 5, Vol. 2, p. 979.
[24]L. H. Toburen, Phys. Rev. A **5**, 2482 (1972).
[25]G. S. Khandelwal, B. H. Choi, and E. Merzbacher, At. Data 1, 103 (1969).
[26]J. D. Garcia, Phys. Rev. A **1**, 280 (1970).
[27]W. Brandt, R. Laubert, and I. Sellin, Phys. Rev. **151**, 56 (1966).
[28]W. Brandt, in Ref. 5, Vol. 2, p. 948.

PHYSICAL REVIEW A VOLUME 7, NUMBER 6 JUNE 1973

Error Bounds on Dynamic Polarizability and Oscillator Strength*

P. T. Gee and K. T. Tang
Department of Physics, Pacific Lutheran University, Tacoma, Washington 98447
(Received 26 January 1973)

Two uniformly convergent series are introduced to give bounded estimates of the dynamic polarizability in the region below as well as above the first resonance line. Upper and lower bounds on the oscillator strength can also be obtained from these approximations. The series are simple and rapidly convergent.

The frequency-dependent (dynamic) polarizability $\alpha(\omega)$, being important in many physical and chemical considerations, has been subjected to intensive study in recent years.[1,2] Here we wish to introduce two approximations for $\alpha(\omega)$. One is uniformly convergent to it from above and the other from below. They have the advantages of being simple and rapidly convergent. Furthermore, the upper and lower bounds of the oscillator strength can also be obtained from these approximations.

The dynamic polarizability is given by the Kramers–Heisenberg dispersion formula

$$\alpha(\omega)=\sum_i \frac{f_i}{\epsilon_i^2-\omega^2} , \tag{1}$$

where f_i is the electric dipole oscillator strength for the transition from the ground state to state i with excitation energy ϵ_i. The summation sign is understood to include integration over the continuum and atomic units are used for all quantities. Expanding Eq. (1) in a Taylor series about the origin, we obtain the Cauchy equation

$$\alpha(\omega)=\sum_{j=0}^{\infty} \mu_j \omega^{2j} , \tag{2}$$

with the Cauchy moments μ_j given by the oscillator-strength sums $S(k)$ defined as

$$\mu_j = S(-2j-2)=\sum_i \frac{f_i}{\epsilon_i^{2j+2}} . \tag{3}$$

The radius of convergence is ϵ_1. The first few Cauchy moments can be determined either experimentally or theoretically. To approximate Eq. (1) with finite number of Cauchy moments, we introduce the following:

$$\alpha_a^n(\omega)=\frac{1}{\epsilon_1^2-\omega^2}\sum_{k=0}^{n} a_{2k}\omega^{2k} , \tag{4}$$

with

$$a_{2k}=\begin{cases} S(-2)\epsilon_1^2 , & k=0 \\ S(-2k-2)\,\epsilon_1^2 - S(-2k) , & k\neq 0 \end{cases} \tag{5}$$

and

$$\alpha_b^n(\omega)=\frac{1}{(\epsilon_1^2-\omega^2)(\epsilon_2^2-\omega^2)}\sum_{k=0}^{n\geq 0} b_{2k}\omega^{2k} , \tag{6}$$

with

$$b_{2k}=\begin{cases} S(-2)\epsilon_1^2\epsilon_2^2 , & k=0 \\ S(-4)\epsilon_1^2\epsilon_2^2-(\epsilon_1^2+\epsilon_2^2)S(-2) , & k=1 \\ S(-2k-2)\epsilon_1^2\epsilon_2^2-(\epsilon_1^2+\epsilon_2^2)S(-2k) & \\ \quad +S(-2k+2) , & k>1 . \end{cases} \tag{7}$$

To study their relationship with $\alpha(\omega)$, we examine the difference functions[3]

$$g_a^n(\omega)=\alpha_a^n(\omega)-\alpha(\omega) \tag{8}$$

and

$$g_b^n(\omega)=\alpha_b^n(\omega)-\alpha(\omega) . \tag{9}$$

Substituting Eqs. (4) and (1) into Eq. (8) and using Eqs. (5) and (3) to simplify the expression,[4] we find

$$g_a^n(\omega)=\frac{\omega^{2n+2}}{\epsilon_1^2-\omega^2}\sum_i \frac{(\epsilon_i^2-\epsilon_1^2)f_i}{\epsilon_i^{2n+2}(\epsilon_i^2-\omega^2)} . \tag{10}$$

Similarly, from Eq. (9), we have

$$g_b^n(\omega)=-\frac{\omega^{2n+2}}{(\epsilon_1^2-\omega^2)(\epsilon_2^2-\omega^2)} \times\sum_i \frac{(\epsilon_i^2-\epsilon_1^2)(\epsilon_i^2-\epsilon_2^2)f_i}{\epsilon_i^{2n+2}(\epsilon_i^2-\omega^2)} . \tag{11}$$